

The Formazanate Ligand as Electron Reservoir: Bis(Formazanate) Zinc Complexes Isolated in Three Redox States^{**}

Mu-Chieh Chang, Thomas Dann, David P. Day, Martin Lutz, Gregory G. Wildgoose, and Edwin Otten*

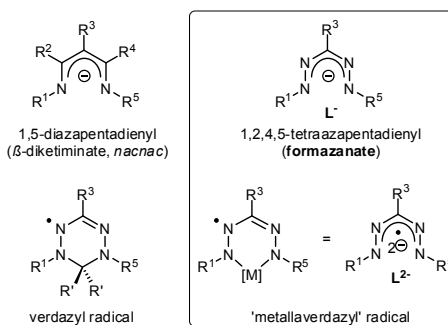
Metal-mediated redox processes are of fundamental importance in a wide variety of bond formation and cleavage reactions. The utility of transition metal catalysts in this type of reactions stems from their ability to switch between two (or more) oxidation states. Recently, there has been increased interest in redox processes that do not occur at the metal centre, but instead take place within the ancillary ligand framework (so-called 'redox-active' or 'non-innocent' ligands).^[1] The use of organic ligands as redox equivalents is of key importance in biological (enzymatic) transformations,^[2] and has been shown to open new reactivity pathways in catalysis.^[1c] The most studied ligands of this class are dithiolenes and dioxolenes, while recent work has focussed on α -diimines^[3] and bis(imino)pyridines.^[4]

A class of ligands that has found widespread utility in the synthesis of metal complexes across the periodic table are the monoanionic β -diketiminates.^[5] These are generally considered as stable ligand scaffolds without involvement in redox-chemistry. Recently, examples of β -diketimate metal complexes were reported in which the ligand was either reduced to a metal-bound di- or trianion,^[6] or oxidized to a neutral radical species.^[7] However, the limited stability of β -diketimate complexes upon changing oxidation state prevents widespread application.^[8]

Formazanates (1,2,4,5-tetraazapentadienyls),^[9] which are close analogues of β -diketiminates, have received comparatively little attention as ligands in coordination chemistry.^[10] The stability of organic 6-membered heterocyclic radicals (verdazyls) that are

derived from formazans prompted us to explore the use of formazanates as potential redox-active ligands (Chart 1). Here we show that zinc complexes with formazanate ligands engage in remarkably facile and reversible redox-chemistry which allows the full characterization of bis(formazanate) L_2Zn complexes in charge neutral, anionic or dianionic redox states.

Chart 1



Bis(formazanate) zinc complexes are readily accessible by protonolysis of Me_2Zn with the neutral ligand precursors $PhNNC(p\text{-tol})NNHPh$ (**1a**) and $PhNNCH^iBu)NNPh$ (**1b**). In the case of formazan **1a**, an immediate colour change from red to intense blue is observed to indicate formation of the bis(formazanate) complex $(PhNNC(p\text{-tol})NNPh)_2Zn$ (**2a**, Scheme 1). Yellow **1b** also reacts immediately with Me_2Zn , but in this case heating to 50 °C overnight was required to obtain full conversion to $(PhNNCH^iBu)NNPh)_2Zn$ (**2b**, Scheme 1). Both complexes are obtained in good yield (>75%) by crystallization as intensely coloured solids. Single crystal x-ray diffraction studies (Figures 1 and S1, pertinent bond distances in Table 2 and S2) reveal a very similar tetrahedral geometry around the central Zn atom.^[11] As is the case in related β -diketimate complexes, full delocalization within the formazanates is indicated by the equivalent N-N and C-N bond lengths in the backbone of each ligand.^[12]

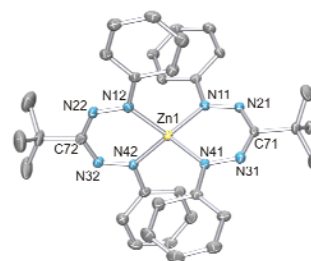


Figure 1. Molecular structure of **2b** showing 50% probability ellipsoids. The hydrogen atoms are omitted for clarity.

[*] Mu-Chieh Chang, Dr. Edwin Otten
Stratingh Institute for Chemistry, University of Groningen
Nijenborgh 4, 9747 AG Groningen, The Netherlands
E-mail: edwin.otten@rug.nl

Dr. Martin Lutz
Bijvoet Center for Biomolecular Research, Crystal and
Structural Chemistry, Utrecht University, Padualaan 8, 3584
CH Utrecht, The Netherlands

Thomas Dann, Dr David P. Day, Dr. Gregory G. Wildgoose
Energy & Materials Laboratory, School of Chemistry,
University of East Anglia, Norwich Research Park, Norwich,
NR4 7TJ, United Kingdom

[**] GGW and DPD thank the European Research Council for funding (ERC Grant Agreement n^o. ERC-StG-307061 PiHOMER). GGW thanks the Royal Society for additional support via a University Research Fellowship. TD thanks the University of East Anglia for financial support via a Dean's studentship. NWO is gratefully acknowledged for funding (Veni grant to EO). We thank Prof. B. de Bruin (University of Amsterdam) for help with VT-EPR experiments and A. Meetsma for useful discussions on the X-ray crystallography.



In order to establish the redox-active nature of the formazanate ligands in compounds **2**, we ran cyclic voltammetry experiments in THF solution with $[\text{Bu}_4\text{N}][\text{B}(\text{C}_6\text{F}_5)_4]$ electrolyte.^[13] Upon scanning in a reductive direction the CV shows two quasi-reversible, single-electron redox processes, labelled system I/I' and II/II' (Figure 2). These correspond to the reversible formation of the radical anions of **2a** and **2b** ($2\text{a}^{\cdot-}$ or $2\text{b}^{\cdot-}$; system I/I') and the corresponding dianions (2a^{2-} or 2b^{2-} ; system II/II') respectively. If the scan direction is reversed after the reductive peak I but before peak II, then the reoxidation of the radical anion ($2\text{a}^{\cdot-}$ or $2\text{b}^{\cdot-}$) is once again observed as peak I' indicating that each redox process is sequential and independent. When the scan rate is varied between 100 and 1000 mVs^{-1} all processes exhibited a linear relationship between peak current and the square root of the voltage scan rate, indicative of diffusion-controlled redox processes. Excellent fits between experiment and digital simulation of the cyclic voltammetry of **2a** and **2b** (Figure 2) yielded optimised values of formal potentials, E^0 , and electron transfer rate constants, k^0 listed in Table 1. Replacing the inductively electron donating *tert*-butyl group with the electron withdrawing *p*-tolyl group on the formazanate ligands has the expected effect on the reduction potentials (Table 1). Interestingly, the one-electron reduction of both bis(formazanate)zinc complexes **2a** and **2b** occurs at more negative potentials ($E^0_{\text{II/II}'} = -1.31$ V vs. $\text{Fc}^{0/+}$, **2a**; -1.57 V vs. $\text{Fc}^{0/+}$, **2b**) than Hicks and co-workers have reported for boron mono(formazanate) compounds ($E^0 \sim -0.9$ V vs. Fc/Fc^+).^[14] This likely reflects the different Lewis acidity of the boron and zinc centres together with a different degree of covalency in the metal-ligand bonding. Cyclic voltammetric characterisation indicates that both the singly-reduced radical anion and the doubly-reduced dianionic states of **2a** and **2b** are synthetically accessible.

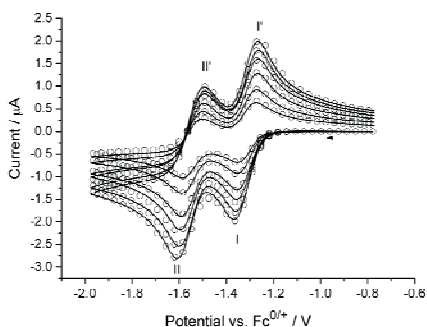


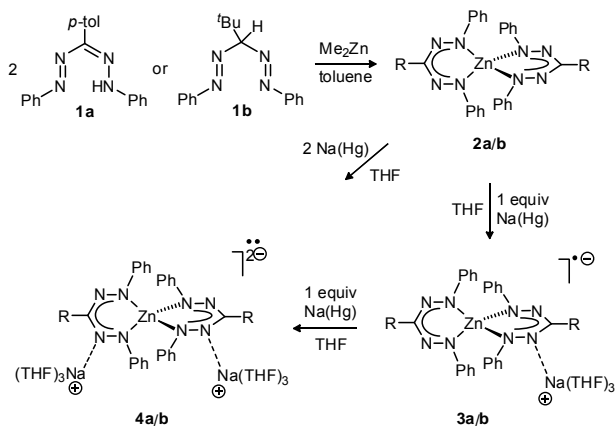
Figure 2. Cyclic voltammograms of a 2.5 mM solution of **2a** in THF (0.1 M $[\text{Bu}_4\text{N}][\text{B}(\text{C}_6\text{F}_5)_4]$) recorded at 100, 200, 400, 600, 800, and 1000 mVs^{-1} . Solid lines = experimental data; open circles = simulated data.

Table 1. Optimised electron transfer parameters determined from digital simulation of experimental voltammetry.

2a	E^0 vs $\text{Fc}^{0/+}$ / V	k^0 / 10^{-2}cms^{-1}
System I/I'	-1.31 ± 0.01	1.25 ± 0.05
System II/II'	-1.55 ± 0.01	0.90 ± 0.05
2b		
System I/I'	-1.57 ± 0.01	1.30 ± 0.05
System II/II'	-1.85 ± 0.02	0.75 ± 0.05

In accordance with the CV data, the chemical reduction of neutral bis(formazanate) complexes **2a** and **2b** could be accomplished by treatment with 1.0 equiv of $\text{Na}(\text{Hg})$ in THF. The

resulting radical species $[\text{Na}(\text{THF})_3][(\text{PhNNC}(\text{R})\text{NNPh})_2\text{Zn}]$ ($\text{R} = p$ -tolyl, **3a**; $\text{R} = t$ -Bu, **3b**) could be isolated as crystalline material by slow diffusion of hexane into the THF solution (Scheme 1). Compounds **3a** and **3b** are NMR silent but show broad EPR signals (g -value ~ 2) both in THF and the solid state (298 and 77K) devoid of observable hyperfine coupling (Figure S3).



Scheme 1. Synthesis of neutral, monoanionic and dianionic bis(formazanate)zinc complexes

The crystallographically determined structures (Figures 3 and S1, pertinent bond distances in Table 2 and S2) show that the tetrahedral $\text{L}_2\text{Zn}^{\cdot-}$ radical anion interacts with a $\text{Na}(\text{THF})_3^+$ cation through one (**3a**) or two (**3b**) nitrogen atoms of a formazanate ligand.^[11] A closer inspection of the metrical parameters within the formazanate backbone reveals that there are two distinctly different ligands in the $\text{L}_2\text{Zn}^{\cdot-}$ fragment. One of the formazanates is very similar to those in the neutral precursors **2** (av. Zn-N: 2.014 Å; N-N: 1.304 Å), while the formazanate that binds the $\text{Na}(\text{THF})_3^+$ has shortened Zn-N (av 1.957 Å) and elongated N-N bond lengths (av 1.363 Å). Thus, the $\text{L}_2\text{Zn}^{\cdot-}$ anion is best described as a Zn^{2+} centre coordinated by a 'normal' monoanionic formazanate (L^-) and a reduced dianionic ligand (L^{2-}). The Zn-coordinated L^{2-} fragment can be considered an inorganic analogue of a verdazyl radical (Chart 1).^[15] The long N-N bonds in the L^{2-} fragment result from the unpaired electron occupying a molecular orbital (SOMO) which has π^* N-N antibonding character (*vide infra*). The observation of two distinct ligand redox states is likely related to electrostatic interactions with the cation, which localizes the additional negative charge. A similar situation is observed in related bis(ligand) complexes: in the case of neutral radical species $[\text{PhB}(\mu\text{-N}^t\text{Bu})_2]_2\text{M}$ ($\text{M} = \text{Al}, \text{Ga}$)^[16] and $(\beta\text{-diketiminate})_2\text{Al}$ ^[17] the unpaired electron is fully delocalized over the spirocyclic structure, while for the radical anions $[\text{PhB}(\mu\text{-N}^t\text{Bu})_2]_2\text{M}^-$ ($\text{M} = \text{Mg}, \text{Zn}$) localized spin density is observed due to interaction with the cation.^[18]

As suggested by the CV measurements, compounds **3** react with an additional equivalent of Na amalgam to give the dianionic complexes $[\text{Na}(\text{THF})_3]_2[(\text{PhNNC}(\text{R})\text{NNPh})_2\text{Zn}]$ ($\text{R} = p$ -tolyl, **4a**; $\text{R} = t$ -Bu, **4b**), of which **4b** was crystallographically characterized (Figure 4, pertinent bond distances in Table 2).^[11] It contains two sodium cations that both interact with two N-atoms of a different formazanate ligand. The presence of an additional electron in both ligands (L^{2-}) is evidenced by the similar bond lengths in **4b**, which are elongated in comparison to the neutral precursor **2b** (Table 2).

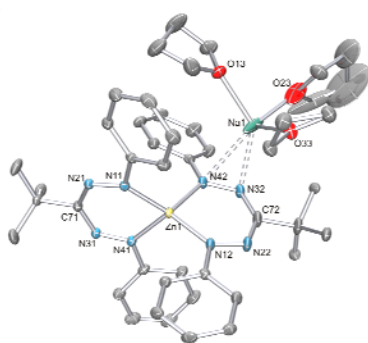


Figure 3. Molecular structure of **3b** showing 50% probability ellipsoids. The hydrogen atoms are omitted for clarity.

Table 2. Selected Bond Distances in **2b**, **3b** and **4b**.

	2b	3b	4b
Zn(1) – N(11)	1.9824(17)	1.9857(16)	1.9793(14)
Zn(1) – N(41)	1.9822(18)	2.0207(16)	1.9839(14)
Zn(1) – N(12)	1.9902(17)	1.9447(16)	1.9696(14)
Zn(1) – N(42)	1.9769(18)	1.9657(16)	1.9952(15)
N(11) – N(21)	1.310(2)	1.313(2)	1.359(2)
N(31) – N(41)	1.307(2)	1.295(2)	1.376(2)
N(12) – N(22)	1.307(2)	1.360(2)	1.355(2)
N(32) – N(42)	1.309(2)	1.370(2)	1.378(2)

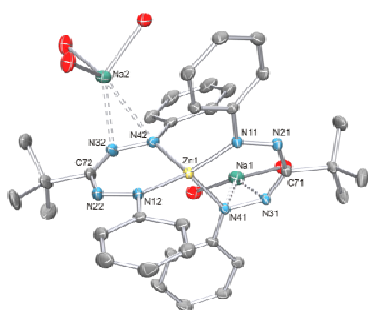


Figure 4. Molecular structure of **4b** showing 50% probability ellipsoids. The carbon atoms of the THF moieties and all hydrogen atoms are omitted for clarity.

EPR spectra of diradicals^[19] **4a** and **4b** in frozen THF solution (77K) are very similar and show features indicative of randomly oriented triplets ($g = 2.0028$) with characteristic half-field ($\Delta m_s = 2$) signals (Figure 5). The zero-field splitting parameters $D = 11.6 \times 10^{-3}$ and $11.5 \times 10^{-3} \text{ cm}^{-1}$ from the EPR spectra for **4a** and **4b**, respectively, are somewhat smaller than those in the neutral triplet diazabutadiene complex $[\text{Bu}_2\text{DAB}]_2\text{Zn}$ ($23.1 \times 10^{-3} \text{ cm}^{-1}$),^[20] and comparable to D -values found for purely organic phenylene-linked bis(radical) compounds (radical = semiquinone,^[21] verdazyl),^[22] which range between ca. $4\text{--}10 \times 10^{-3} \text{ cm}^{-1}$. It should be noted that although metal complexes with coordinated verdazyl radicals have

been prepared,^[23] compounds **4** present the first examples of diradical ‘metallaverdazyl’ compounds.

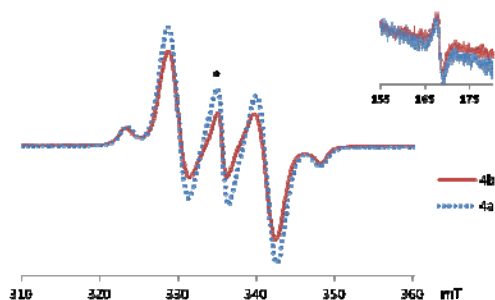


Figure 5. EPR spectra (frozen THF solution) of **4a** and **4b** (asterisk denotes a doublet impurity). Inset: half-field region.

UV-Vis spectroscopy of neutral, anionic and dianionic bis(formazanate) zinc compounds (Figure S2) provides additional evidence for ligand-based reduction and formation of verdazyl-type (L^{2-}) ligands. The neutral compounds **2a** and **2b** show single broad absorptions in the visible range at 578 and 536 nm, respectively. The singly reduced compounds **3** have both formazanate (L^-) and one-electron reduced, verdazyl-type (L^{2-}) ligands. As a consequence, they feature new absorption bands at longer (**3a/3b**: 769/755nm) and shorter wavelengths (**3a/3b**: 508/462 nm) due to L^{2-} ; the position of these bands is similar to that observed in organic (Kuhn-type) triarylverdazyls.^[24] In addition, a weakened and bathochromically shifted absorption is observed which is attributed to the L^- fragment in **3a/b**. For compounds **4a** and **4b**, the intensity of the low and high energy absorptions due to the L^{2-} fragment is increased relative to the singly reduced species **3**. The most prominent absorptions in the visible range are at 510/798 (**4a**) and 436/755 nm (**4b**) in agreement with the presence of only reduced formazanate (verdazyl-type) ligands.

DFT calculations were carried out to examine the electronic structure of the complexes described here. The crystallographically determined bond lengths and angles are reproduced accurately by (unrestricted) B3LYP/6-31G(d) calculations using Gaussian09 starting from the X-ray coordinates. However, geometry optimization of the ‘free’ radical anions **3** at the UB3LYP/6-31G(d) level of theory resulted in structures in which the SOMO is delocalized over both ligands. For example, in **3a_{calc}** the diagnostic N-N bond lengths are all equivalent at $\sim 1.322 \text{ \AA}$, in between the short (L^- : av 1.304 \AA) and long N-N bonds (L^{2-} : av 1.361 \AA) observed experimentally. When the counteranion $[\text{Na}(\text{THF})_3]^+$ that is present in the crystal structure determination is included in the computations, the unpaired electron is localized (see Figure 6 for **3a_{calc}**). This is in agreement with the experimental data and suggests that electrostatic effects are responsible for this localization. The calculated hyperfine interactions with the ^{14}N nuclei are small in **3a_{calc}** ($< 2.1 \text{ G}$), which likely accounts for the broad, featureless EPR signals observed experimentally.

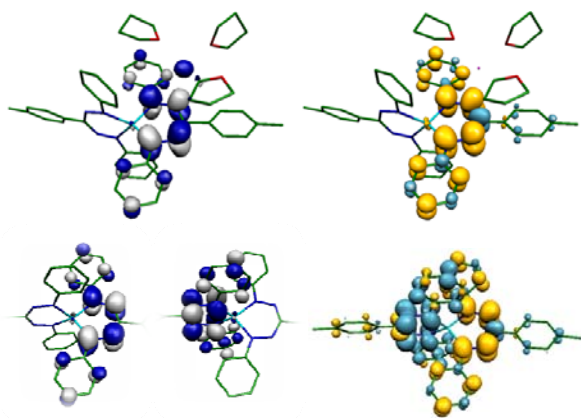


Figure 6. Top: SOMO (left) and spin density plot (right) for **3a**_{calc.} Bottom: Two ligand-centered SOMOs for the BS(1,1) solution (truncated structures, left) and spin density plot (right) for **4a**_{calc.}

For the diradicals **4**, geometry optimizations of the L_2Zn^2 fragment in the absence of counteranions converges at structures that have two (virtually) identical L^2 ligands with elongated N-N bond lengths of ca. 1.346 Å, which is somewhat shorter than those observed experimentally for **4b** (av. 1.367 Å). Broken-symmetry DFT calculations^[25] show two ligand-based unpaired electron spins that are antiferromagnetically coupled ($J_{\text{calc}} = -7.9 \text{ cm}^{-1}$) to give a singlet diradical ground state (Figure 6). The calculated spin density in diradical **4a**_{calc} indicates that the unpaired electrons are located at the nitrogen atoms of the ligands, with some contribution of the aromatic substituents. To verify experimentally the ground state of **4a**, preliminary EPR studies were carried out in the temperature range of 6-60K (THF glass) to determine the temperature dependence of the EPR signal intensity (I). A plot of $I \times T$ vs. T shows that $I \times T$ decreases upon lowering the temperature (Figure S4). This behaviour is indicative of a singlet diradical ground state,^[19] thus corroborating our computational results. Although singlet biradical species like **4** are rare, Roesky and co-workers recently reported a dicarbene zinc compound for which the singlet diradical was calculated to be lower in energy than the triplet by ~ 4 kcal/mol.^[26]

In conclusion, we have shown that complexes with formazanate ligands give rise to reactivity that is not accessible with their β -diketiminato congeners. Bis(formazanate) zinc complexes engage in remarkably facile reductive chemistry to give isolable one- and two-electron reduction products of L_2Zn , the stability of which results from the ‘metallaverdazyl’-type structures obtained. The use of coordinated formazanates as reversible electron reservoir in (catalytic) reactions is currently under investigation in our laboratory.

Experimental Section

(PhNNC(*p*-tolyl)NNPh)₂Zn (2a). A 1.2 M solution of Me_2Zn in toluene (0.82 mL, 0.98 mmol) was added slowly to a suspension of PhNNC(*p*-tolyl)NNPh (620 mg, 1.97 mmol) in 10 mL of toluene at room temperature. The mixture was stirred for 2 h after which the colour had changed to intense blue. The volatiles were removed in vacuo and the residue was subsequently extracted into a hot 3:1 hexane/toluene mixture. Slow cooling of the clear dark blue solution to -30 °C for 2 days afforded 552 mg dark violet crystals of (PhNNC(*p*-tolyl)NNPh)₂Zn·(toluene)_{0.5} (0.75 mmol, 76%). ¹H NMR (200 MHz, C₆D₆, 25 °C) δ 8.42 (d, 2H, $J = 7.9$, *p*-tolyl CH), 7.70 (d, 4H,

$J = 7.8$, Ph *o*-H), 7.29 (d, 2H, $J = 7.9$, *p*-tolyl CH), 6.81 (t, 4H, $J = 7.7$, Ph *m*-H), 6.66 (t, 2H, $J = 7.4$, Ph *p*-H), 2.25 (s, 3H, *p*-tolyl CH₃). ¹³C NMR (50.4 MHz, C₆D₆, 25 °C) δ 152.8 (Ph *ipso*-C), 144.0 (NCN), 137.6 (*p*-tolyl *ipso*-C), 137.1 (*p*-tolyl CMe), 129.7 (Ph *m*-CH), 129.6 (*p*-tolyl CH), ~127.5 (overlapped, Ph *p*-CH), 126.4 (*p*-tolyl CH), 120.2 (Ph *o*-CH), 21.2 (*p*-tolyl CH₃). Anal. Calcd for C_{43.5}H₃₈N₆Zn: C, 70.78; H, 5.19; N, 15.18. Found: C, 70.74; H, 5.21; N, 15.13.

[Na(THF)₃]⁺[(PhNNC(*p*-tolyl)NNPh)₂Zn]⁻ (3a). One leg of a double-schlenk flask was charged with **2a** (750 mg, 1.02 mmol), Na(Hg) (2.447 wt% Na, 1222 mg, 1.30 mmol) and 15 mL of THF. The reaction mixture was stirred for overnight, filtered and reduced to half of the original volume. Slow diffusion of hexane (15 mL) into the THF solution precipitated 658 mg of [Na(THF)₃]⁺[(PhNNC(*p*-tolyl)NNPh)₂Zn]⁻ as brown crystalline material (0.707 mmol, 69%). Anal. Calcd for C₅₂H₅₈N₈NaO₃Zn: C, 67.05; H, 6.28; N, 12.03. Found: C, 66.84; H, 6.25; N, 11.90.

[Na(THF)₃]⁺₂[(PhNNC(*p*-tolyl)NNPh)₂Zn]²⁻ (4a). A mixture of solid **2a** (50 mg, 0.068 mmol) and 149.5 mg Na/Hg (2.447 wt%, 3.7 mg Na, 0.159 mmol) was prepared. With stirring, 7 mL of THF was added at room temperature. After stirring the reaction mixture one week, 28 mL of pentane was added at room temperature to precipitate the product. The supernatant was decanted and the crystalline product washed with pentane to give 30.0 mg of [Na(THF)₃]⁺₂[(PhNNC(*p*-tolyl)NNPh)₂Zn]²⁻ as green crystalline material (0.026 mmol, 39%). Anal. Calcd for C₆₄H₈₂N₈Na₂O₆Zn: C, 65.55; H, 7.06; N, 9.57. Found: C, 65.53; H, 6.89; N, 9.87.

Received: ((will be filled in by the editorial staff))

Published online on ((will be filled in by the editorial staff))

Keywords: radical ligands · zinc complexes · metallaverdazyl · formazanate · redox chemistry

- [1] a) Chirik, P. J.; Wieghardt, K. *Science* **2010**, *327*, 794; b) Dzik, W. I.; van der Lugt, J. I.; Reek, J. N. H.; de Bruin, B. *Angew. Chem. Int. Ed.* **2011**, *50*, 3356; c) Lyaskovskyy, V.; de Bruin, B. *ACS Catal.* **2012**, *2*, 270.
- [2] Que, L.; Tolman, W. B. *Nature* **2008**, *455*, 333.
- [3] Tsurugi, H.; Saito, T.; Tanahashi, H.; Arnold, J.; Mashima, K. *J. Am. Chem. Soc.* **2011**, *133*, 18673.
- [4] a) Bouwkamp, M. W.; Bowman, A. C.; Lobkovsky, E.; Chirik, P. J. *J. Am. Chem. Soc.* **2006**, *128*, 13340; b) Bart, S. C.; Chlopek, K.; Bill, E.; Bouwkamp, M. W.; Lobkovsky, E.; Neese, F.; Wieghardt, K.; Chirik, P. J. *J. Am. Chem. Soc.* **2006**, *128*, 13901; c) Darmon, J. M.; Stieber, S. C. E.; Sylvester, K. T.; Fernández, I.; Lobkovsky, E.; Semproni, S. P.; Bill, E.; Wieghardt, K.; DeBeer, S.; Chirik, P. J. *J. Am. Chem. Soc.* **2012**, *134*, 17125; d) Tondreau, A. M.; Stieber, S. C. E.; Milsman, C.; Lobkovsky, E.; Weyhermüller, T.; Semproni, S. P.; Chirik, P. J. *Inorg. Chem.* **2013**, *52*, 635.
- [5] Bourget-Merle, L.; Lappert, M. F.; Severn, J. R. *Chem. Rev.* **2002**, *102*, 3031.
- [6] a) Avent, A. G.; Hitchcock, P. B.; Khvostov, A. V.; Lappert, M. F.; Protchenko, A. V. *Dalton Trans.* **2004**, 2272; b) Eisenstein, O.; Hitchcock, P. B.; Khvostov, A. V.; Lappert, M. F.; Maron, L.; Perrin, L.; Protchenko, A. V. *J. Am. Chem. Soc.* **2003**, *125*, 10790; c) Avent, A. G.; Khvostov, A. V.; Hitchcock, P. B.; Lappert, M. F. *Chem. Commun.* **2002**, 1410.
- [7] Khusniyarov, M. M.; Bill, E.; Weyhermüller, T.; Bothe, E.; Wieghardt, K. *Angew. Chem. Int. Ed.* **2011**, *50*, 1652.
- [8] a) Basuli, F.; Kilgore, U. J.; Brown, D.; Huffman, J. C.; Mindiola, D. J. *Organometallics* **2004**, *23*, 6166; b) Hamaki, H.; Takeda, N.; Tokitoh, N. *Organometallics* **2006**, *25*, 2457; c) Bai, G.; Wei, P.; Stephan, D. W. *Organometallics* **2006**, *25*, 2649; d) Tomson, N. C.; Arnold, J.; Bergman, R. G. *Organometallics* **2010**, *29*, 5010.
- [9] Nineham, A. W. *Chem. Rev.* **1955**, *55*, 355.
- [10] a) Gilroy, J. B.; Patrick, B. O.; McDonald, R.; Hicks, R. G. *Inorg. Chem.* **2008**, *47*, 1287; b) Gilroy, J. B.; Ferguson, M. J.; McDonald,

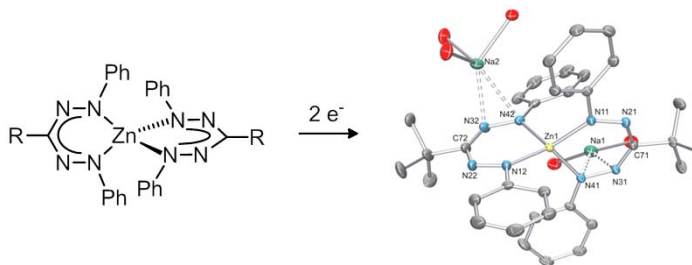
- R.; Hicks, R. G. *Inorg. Chim. Acta* **2008**, *361*, 3388; c) Hong, S.; Hill, L. M. R.; Gupta, A. K.; Naab, B. D.; Gilroy, J. B.; Hicks, R. G.; Cramer, C. J.; Tolman, W. B. *Inorg. Chem.* **2009**, *48*, 4514.
- [11] CCDC 972163-972167 contains the supplementary crystallographic data for this paper. These data can be obtained free of charge from The Cambridge Crystallographic Data Centre via www.ccdc.cam.ac.uk/data_request/cif
- [12] a) Cheng, M.; Moore, D. R.; Reczek, J. J.; Chamberlain, B. M.; Lobkovsky, E. B.; Coates, G. W. *J. Am. Chem. Soc.* **2001**, *123*, 8738; b) Tsai, Y.-C. *Coord. Chem. Rev.* **2012**, *256*, 722.
- [13] Geiger, W. E.; Barrière, F. *Acc. Chem. Res.* **2010**, *43*, 1030.
- [14] Gilroy, J. B.; Ferguson, M. J.; McDonald, R.; Patrick, B. O.; Hicks, R. G. *Chem. Commun.* **2007**, 126.
- [15] Hicks, R. G. *Verdazyls and Related Radicals Containing the Hydrazyl [R2N-NR] Group*; In *Stable Radicals*; John Wiley & Sons, Ltd: 2010, p 245.
- [16] Chivers, T.; Eisler, D. J.; Fedorchuk, C.; Schatte, G.; Tuononen, H. M.; Boere, R. T. *Chem. Commun.* **2005**, 3930.
- [17] Moilanen, J.; Borau-Garcia, J.; Roesler, R.; Tuononen, H. M. *Chem. Commun.* **2012**, *48*, 8949.
- [18] Chivers, T.; Eisler, D. J.; Fedorchuk, C.; Schatte, G.; Tuononen, H. M.; Boeré, R. T. *Inorg. Chem.* **2006**, *45*, 2119.
- [19] Abe, M. *Chem. Rev.* **2013**.
- [20] Gardiner, M. G.; Hanson, G. R.; Henderson, M. J.; Lee, F. C.; Raston, C. L. *Inorg. Chem.* **1994**, *33*, 2456.
- [21] a) Shultz, D. A.; Boal, A. K.; Driscoll, D. J.; Kitchin, J. R.; Tew, G. N. *J. Org. Chem.* **1995**, *60*, 3578; b) Shultz, D. A.; Boal, A. K.; Farmer, G. T. *J. Org. Chem.* **1998**, *63*, 9462.
- [22] a) Fico, R. M.; Hay, M. F.; Reese, S.; Hammond, S.; Lambert, E.; Fox, M. A. *J. Org. Chem.* **1999**, *64*, 9386; b) Gilroy, J. B.; McKinnon, S. D. J.; Kennepohl, P.; Zsombor, M. S.; Ferguson, M. J.; Thompson, L. K.; Hicks, R. G. *J. Org. Chem.* **2007**, *72*, 8062.
- [23] a) Barclay, T. M.; Hicks, R. G.; Lemaire, M. T.; Thompson, L. K. *Inorg. Chem.* **2001**, *40*, 6521; b) Brook, D. J. R.; Yee, G. T.; Hundley, M.; Rogow, D.; Wong, J.; Van-Tu, K. *Inorg. Chem.* **2010**, *49*, 8573; c) Anderson, K. J.; Gilroy, J. B.; Patrick, B. O.; McDonald, R.; Ferguson, M. J.; Hicks, R. G. *Inorg. Chim. Acta* **2011**, *374*, 480.
- [24] Kuhn, R.; Trischmann, H. *Monatsh. . Chemie* **1964**, *95*, 457.
- [25] Neese, F. *Coord. Chem. Rev.* **2009**, 253, 526.
- [26] Singh, A. P.; Samuel, P. P.; Roesky, H. W.; Schwarzer, M. C.; Frenking, G.; Sidhu, N. S.; Dittrich, B. *J. Am. Chem. Soc.* **2013**, *135*, 7324.

Entry for the Table of Contents (Please choose one layout)

Redox Non-Innocent Ligands

M.-C Chang, T. Dann, D. P. Day, M. Lutz, G. G. Wildgoose, E. Otten* _____ **Page – Page**

The Formazanate Ligand as Electron Reservoir: Bis(Formazanate) Zinc Complexes Isolated in Three Redox States



N is better than C: Bis(formazanate) zinc complexes show sequential and reversible redox-chemistry, in which the formazanate ligands are reduced to ‘metalaverdazyl’ radicals. The structural features of these ligands are very similar to well-known β -diketiminates, but the nitrogen-rich (NNCNN) backbone of formazanates opens the door to redox-chemistry not easily accessible otherwise.